

# ECOLOGY, ENVIRONMENT AND CONSERVATION

## VOL. 28 (February Suppl. Issue) : 2022

### CONTENTS

- S1–S5 Parental investment of adult Barn swallow *Hirundo rustica rustica* at nestling feeding in the urban locality of El Bouni (Northeast, Algeria)  
—*Dadci Walid, Sakraoui Rym, Boukheroufa Mehdi, Abdallah Khadidja Wissal, Sakraoui Ferial and Tahar Ali*
- S6–S13 Land-Use/ Land-Cover Changing Trends and their Relation to Landslides: A Case Study of Hali-Elain Badulla District, Sri Lanka  
—*A.M.R.N.K. Alahakoon, K.L. Thisara Sathsara, Udara S.P.R. Arachchige and Shyamantha Subasinghea*
- S14–S20 Regional and Seasonal Variations of Polychlorinated Biphenyls (PCBs) in Water of Shatt AL-Arab River, Iraq  
—*Rafid A.T. Al-Zabad, Ayad H.D. Al-Khafaji and Hamid T. AL-Saad*
- S21–S27 Synthesis and Characterization of Nanocellulose from *Cladophora* sp.  
—*S.W. Suciayati, P. Manurung, Junaidi, S. Sembiring and R. Situmeang*
- S28–S34 A Teacher's Perception of Green Building Technology: Implications to Sustainable Construction and Environmental Education in Anambra State, Nigeria  
—*Daniel Uchenna Chukwu, Hyginus Osita Omeje, Godwin Keres Okereke, Chinwe Patricia Eze and Ikechukwu Chidiebere Odogwu*
- S35–S40 Antitumor and antioxidant activity of *Aloe Vera* leaf gel extract  
—*Worood Kamil Shalash*
- S41–S45 Effect of Polyphenol Fraction Exposure of *Aloe vera* on the Change in Cortisol of Koi Fish (*Cyprinus carpio*) as Stress Response  
—*Sri Andayani, M Sulaiman Dadiono, Widya Tri Elwira, Husna Nabila, Rodhyansyah, Nelvan Subayu and Ashari Fahrurrozi*
- S46–S51 Regulatory Framework for the Disposal and Management of Personal Protective equipment (PPE) During Covid-19 in Bangladesh  
—*Farhana Helal Mehtab, Md. Safiullah and Md. Arif Mahmud*
- S52–S58 Solar Cell as Energy Chlorinator for Disinfection of Flowing Water  
—*Beny Suyanto, Denok Indraswati, Tuhu Pinardi and Sujangi*
- S59–S61 Production Performance of Broiler Chicken Supplemented with *Lactobacillus plantarum* and *Lactobacillus casei* Incubated in Different Medium Infusion  
—*Nabila Hanina Hibatul Haqqi, Fatihah Istafaro Maulidiya, Galuh Hesti Dwi Indrawati<sup>1</sup>, Wenny Nur Azizah, Herinda Pertiwi and Loh Teck Chwen*
- S62–S73 Motivators and Inhibitors of Green Building Technology Integration and Advancement: Nigerian Lecturers' perspective  
—*D. U. Chukwu, H. O. Omeje, G. K. Okereke, B. A. Omeje, A. A. Okekpa and J. A. Okereke*
- S74–S78 The Impact of Electromagnetic Pollution on Human Health and Environment: Recommendation for an Effective Regulatory Framework in Bangladesh  
—*Arif Mahmud*
- S79–S84 Differences effect of red and big white ginger extract as anti-inflammatory agents by *In vitro*  
—*E.B. Aksono, T.D.K. Wungu, C.H. Wijaya, R.R.F. Sarassina, N. Hidayatik, H. Pertiwi and N. Puspitasari*
- S85–S92 Visualization of Coral Reef Cover with Photogrammetry Method at Coastal Waters of Lemon Island, Manokwari, Indonesia  
—*Dimas Algutomo, Ricardo F. Tapilatu, and Aradea Bujana Kusuma*

# Synthesis and Characterization of Nanocellulose from *Cladophora* sp.

S. W. Suciwati<sup>1,\*</sup>, P. Manurung<sup>2,\*</sup>, Junaidi<sup>2</sup>, S. Sembiring<sup>2</sup> and R. Situmeang<sup>3</sup>

<sup>1</sup>Doctoral Program of Mathematics and Natural Science, University of Lampung, Bandar Lampung 35145, Indonesia

<sup>2</sup>Department of Physics, University of Lampung, Bandar Lampung - 35145, Indonesia

<sup>3</sup>Department of Chemical, University of Lampung, Bandar Lampung -35145, Indonesia

(Received 20 May, 2021; Accepted 13 July, 2021)

## ABSTRACT

*Cladophora* has a unique cellulose structure and is easy to extract. In this study, ClaNC was isolated from freshwater green algae (*Cladophora glomerata*) that thrived in swamps, using hydrochloric acid (HCl) hydrolysis. This study was conducted on the changes of chemical composition, morphology and structure of ClaNC through FTIR, XRD, SEM, and TEM. Lignin removal (peak 1535 cm<sup>-1</sup>) was effective after HCl hydrolysis, but bands 1028 and 894 cm<sup>-1</sup> confirmed the identity of the chemical composition of *Cladophora glomerata* lettuce which was not lost even at nano-scale. XRD analysis revealed the ClaNC crystal index was 94.0% with a preferred orientation in the lattice plane of I $\alpha$  [110] and I $\beta$  [200]. The surface morphology of *Cladophora* raw material is rod-shaped as shown by SEM, with an average diameter of 21.3 ( $\pm$  1.01)  $\mu$ m, whereas ClaNC refers to nanofibrils with an average diameter of 30.6 ( $\pm$  0.85) nm as shown by TEM.

**Key words:** *Cladophora*, Freshwater green algae, Nanocellulose, Nanofibril

## Introduction

Cellulose is a natural polymer that is abundantly available on the earth and is a prime candidate as a substitute for petroleum-based raw materials. Its nature is easily biodegradable, sustainable, biocompatible, and its availability is abundant, making cellulose a very special material among scientists to be developed as an advanced material. Various natural sources have been synthesized for the production of cellulose/nano cellulose, ranging from seasonal forests, agricultural residues, algae, and microorganisms such as bacteria. The abundance of nanocellulose precursors gives preference to certain types, but it would be preferable to produce nanocellulose from fast-growing plants rather than from slow-growing plants due to economic and eco-

logical benefits. Synthesis of nanocellulose will break down the hierarchical structure of cellulose into the basic building blocks of cell walls, where for plant-based cellulose materials this destruction forms so-called nanocrystals, nanowhiskers, nanofibrils, and nanofibers without changing the macroscopic properties of cellulose. Top-down synthesis methods involving enzymatic/chemical/physical methods as well as combinations of these methods for the isolation of nanocellulose have been extensively investigated (Nandi and Guha, 2018).

The structure of cellulose is formed by hydrogen bonds between a network of hydroxyl groups, which are repeated 1,4-linked anhydrous-D-glucose units linked by 1-4 glycosidic bonds (Moon *et al.*, 2011). Cellulose is composed of crystalline polymorphs that can be isolated for various applications of

Corresponding author's email: sri.wahyu@fmipa.unila.ac.id

<sup>1</sup>Ph.D Student

cellulose-based biomaterials with various special characteristics formed by the assembly of crystals through hydrogen bonds (George and Montemagno, 2017; Tayeb *et al.*, 2018). The separation of cellulose fibers into basic microfibrils on the nanoscale or nanofibrils/microcrystalline is of great interest due to its unique optical, rheological, and mechanical properties (Zhu *et al.*, 2011; Hua *et al.*, 2014). Separating cellulose fibers uniformly into nanocrystalline cellulose (CNC), with its large aspect ratio is difficult. Nanocrystalline cellulose (CNC) is a nanometer-sized cellulose fiber with a rod or needle-like structure and a crystalline phase. The length and width of the CNC particles depend on the source of the nanocellulose, but are generally about 1–10 nm in width and hundreds of nanometres in length (Habibi *et al.*, 2010; Pereira *et al.*, 2020).

Various methods successfully synthesize nanocellulose precursors to obtain micrometer or nanometer -sized pure cellulose (Trache *et al.*, 2016; Camacho *et al.*, 2017). Cellulose synthesis using algal precursors showed high levels of crystallinity, larger surface area and pore content than other cellulose samples (Mihrianyan *et al.*, 2004). Algae from the *Cladophora* family are plants that are easily found in water (fresh or saline) and wetlands. Reproduction of *Cladophora* sp. very fast, thus becoming a problem in the aquatic environment due to the excessive production of carbon dioxide as a result of photosynthesis of *Cladophora* sp. (Mihrianyan, 2011). The unique characteristics of *Cladophora* sp. as well as its advantages, is a primary candidate for synthesis as a CNC.

Proper treatment during synthesis is very important because the raw material besides containing cellulose also contains hemicellulose and lignin which must be removed, as both are non-crystalline fibers. A top-down method with a hydrolysis scheme can be used to remove lignin, hemicellulose, wax, and oil that covers the outer surface of the fiber cell wall (Abraham *et al.*, 2011; Moreno *et al.*, 2018). Acid hydrolysis with a combination of microfluidization or ultrasound treatment is a commonly used chemical method to isolate crystal phases (Xiang *et al.*, 2016; Karim *et al.*, 2014) in cellulose due to its simplicity and low energy consumption. Special properties such as non-toxic, biodegradability, renewable, high strength and modulus, low density, reactive surface, and large specific surface area support the potential for CNC applications (Giese *et al.*, 2015; Bagheri *et al.*, 2017; Lee *et al.*, 2019). These properties are highly dependent on the cellulose source, pre-treatment,

isolation method, and extraction treatment conditions (Dufresne, 2013; Brinchi *et al.*, 2013). The acid hydrolysis process consists of crushing and removing amorphous components by leaving crystal segments (Moberg *et al.*, 2017). This occurs because the contact of the fiber with a strong acid solution allows the amorphous region to decompose easily, and because the kinetics of hydrolysis in this region is faster than that of crystals, so the hydrolyzed material becomes more permeable (Kallel *et al.*, 2016).

*Cladophora* sp. is a species of green algae that has the potential to be synthesized and extracted as nanometer-sized crystalline cellulose (Sucaldito and Camacho, 2017; Xiang *et al.*, 2016). Its abundant richness can be a problem (algae blooms) if the environment in which it lives strongly supports algal growth. Regarding minimizing environmental problems, some literature mentions that CNC products from *Cladophora* sp. have high crystalline properties compared to woody plants (Beads *et al.*, 2018; Xiang *et al.*, 2016; Mihrianyan, 2011). Even from the same species, the CNC products produced can be very different (Suciyati *et al.*, 2021), so in this study, we aimed to obtain optimal CNC characteristics from *Cladophora* sp. growing in swamps. A systematic extraction process was performed for the CNC synthesis of *Cladophora* sp. using the hydrolysis method. The CNC potentials extracted from these algae were studied comprehensively in terms of functional assembly, morphology, structure, and crystallinity. CNC characterization was performed using Fourier Transform Infrared (FTIR), X-Ray Diffractograms (XRD), Scanning Electron Microscope (SEM), and Transmission Electron Microscope (TEM).

## Experimentals

### Materials and Methods

*Cladophora* glomerata taken from a swamp on the banks of the Musi river in February 2021. The samples were cleaned by washing them in running water and then dried. The chemicals used for cellulose synthesis are NaClO<sub>2</sub>, NaOH, HCl, glacial acetic acid purchased from Sigma Aldrich (Merck). Preparation of *Cladophora* glomerata done by washing, drying, and mixing. Isolation and extraction processes generally develop procedures (Xiang *et al.*, 2016) with modifications. Examples of *Cladophora* sp. (3 g) was bleached with a mixed solution of sodium acetate buffer (30 ml, pH 4–5) with NaClO<sub>2</sub> (1.2 g) for 3 h in a water bath (60 °C). The solids were sepa-

rated and washed with deionized water to neutral (pH ~7) using a centrifuge at 4000 rpm for 20 min. The centrifuged treatment was repeated 6 times to reduce the acid content, thereafter the solid was mixed with 0.5 M NaOH (36 mL) and heated in a water bath (60 °C) overnight. The solid was then washed with deionized water to remove alkaline residue using a centrifuge, then dried. Once dry, the samples were mixed with 5% HCl (18 ml) then heated (90 °C) to boiling, and then left overnight at room temperature. Cellulose was then separated by washing to neutral (pH ~7), and freeze-drying. To obtain cellulose powder, filtration was performed with a 200 mesh sieve.

### Characterizations

Sample characterization was performed using Agilent's FTIR Cary 630 brand, with biomass components determined non-destructively through IR intermediate spectrum absorption. The data recording range was 650–4000  $\text{cm}^{-1}$  for 32 scans. Characterization of chemical structures with identified FTIR functional groups and infrared absorption band intensities in samples. X-ray diffraction (XRD) measurements were performed by XRD type PANalytical: X'Pert Pro diffraction analyzer. The diffracted intensity of Cu K-alpha radiation ( $k = 1.540598\text{\AA}$ ) at 40 kV and 30 mA was measured in a  $2\theta$  range of  $5^\circ$ – $90^\circ$ . Dari data difraktogram XRD ini dapat diketahui indeks kristalinitas CNC melalui metode empiric berbantuan persamaan Segal crystallinity index (CI) that was calculated by using the following equation (Xiang *et al.*, 2016),

$$CI = \frac{I_{max} - I_{min}}{I_{min}} \times 100\% \quad (1)$$

where  $I_{max}$  is the intensity of the highest peak at a  $2\theta$  angle close to  $22.8^\circ$ , and  $I_{min}$  is the minimum intensity at a  $2\theta$  angle close to  $18^\circ$  for cellulose I. The highest intensity peak is corresponding to a crystalline peak, while the minimum intensity is the intensity of the background scattered corresponding to the amorphous peak.

Furthermore, to calculate the crystallite size, the Scherrer equation is used,

$$L = \frac{K\lambda}{B \cos \theta} \quad (2)$$

where  $L$  is the width (length) in  $\text{\AA}$ ,  $K$  is the shape correction factor (0.9),  $\lambda$  is the wavelength of the radiation ( $1.540598\text{\AA}$ ),  $B$  is the FWHM of the highest dif-

fraction peak (rad), and  $\theta$  is half of the highest angle of the peaks in the  $2\theta$  range.

Surface morphology of *Cladophora glomerata* nanocellulose (ClaNC) analyzed using SEM-EDX ZEISS EVO MA 10, Germany. Images from SEM-EDX were taken at several magnification values. Further analysis of the internal crystal structure of the ClaNC was observed based on transmission electron micrographs collected using the TEM Jeol Jem-1400, Japan.

## Results and Discussion

### FTIR characterization of cellulose

The chemical structural characteristics and functional groups of cellulose are in the wavelength range of 400–4000  $\text{cm}^{-1}$ , i.e. the area of the absorption band involving the transition between the vibrational energy state and the rotation of the molecular substrate (Trache *et al.*, 2016; Fuller *et al.*, 2018). Fig. 2 shows the characteristics of the functional group of the algae *Cladophora glomerata* before and after synthesis. In *Cladophora glomerata* cellulose, the presence of stretching and vibration of the OH functional group is beneficial in the formation of cellulose composites, either with synthetic polymers or biopolymers, and even the formation of cellulose-based hybrid materials (Keshavarzi *et al.*, 2015; Mun *et al.*, 2017; Zhou *et al.*, 2019).

The FTIR pattern (Fig. 1) can show chemical changes due to the raw material extraction process of *Cladophora glomerata* into ClaNC. The 1535  $\text{cm}^{-1}$

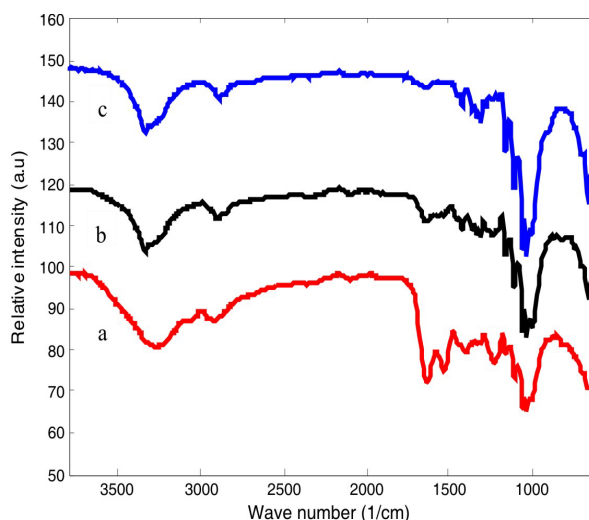


Fig. 1. FTIR spectra of (a) raw material, (b) bleach-alkali-treated, (c) ClaNC from *Cladophora* sp.

band (raw material) is associated with aromatic lignin stretching and the  $1222\text{ cm}^{-1}$  band corresponds to the C-O-C (aryl-alkyl ether) stretching. Both of these bands still exist after alkali and bleaching treatments indicating that the lignin has not been completely removed, but the peaks of the bands effectively disappear after acid hydrolysis treatment. The absorption bands in the  $1640$  and  $2914\text{ cm}^{-1}$  regions are due to the stretching of the O-H group and the C-H group in the water molecule. While the peak of  $3400\text{--}3272\text{ cm}^{-1}$  is aimed at O-H stretching and water absorption. It is very difficult to remove water from cellulose due to the cellulose-water interaction, so this strip remains thereafter hydrolysis treatment. Two bands  $1028$  and  $894\text{ cm}^{-1}$  are caused by C-O and C-H vibration stretching from carbohydrate oscillations, which are related to native cellulose (Sucaldito and Camacho, 2017). This special strip is present to confirm the identity of cellulose extracted from *Cladophora glomerata*. In addition, the presence of this strip was maintained in ClaNC indicating that the chemical composition of cellulose was not lost even in its nanocrystalline form. Peaks in the  $1500\text{--}1660\text{ cm}^{-1}$  range indicate the presence of protein (Jagadeesh *et al.*, 2011; Xiang *et al.*, 2016), and disappear after hydrolysis treatment; its absence indicates that *Cladophora glomerata* after extraction contained only undetectable amounts of protein.

### X-ray diffraction of cellulose *Cladophora*

The crystallinity of the sample powder was analyzed with an X-ray diffract meter and shown in Fig. 2. The spectrum generated by the XRD diffraction analyzer using a step measurement of  $0.017^\circ$ , from

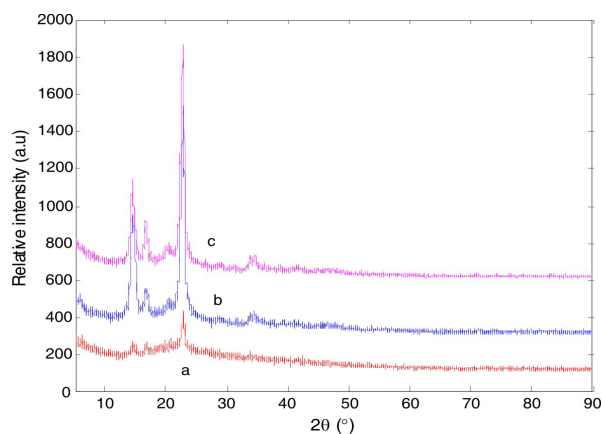


Fig. 2. XRD pattern of (a) raw material, (b) bleach-alkali-treatment, (c) ClaNC, from *Cladophora* sp.

the X-ray radiation source: Cu-K $\alpha$  with wavelength  $1.540598\text{ \AA}$ .

Unlike hemicellulose and lignin, cellulose has a crystalline structure in nature formed by hydrogen bonds and Van der Waals forces between molecules. XRD characterization diffractograms provide information on the crystal structure of *Cladophora glomerata* with the bulk being cellulose I (crystalline cellulose) (Camacho *et al.*, 2013). Cellulose I consists of I $\alpha$  (triclinic structure) and I $\beta$  (monoclinic structure) where the I $\alpha$  structure is more dominant in polymorphs from algal sources. XRD characterization method was used to calculate the crystallinity index of algae samples. XRD patterns for the various stages of cellulose extraction from *Cladophora glomerata* in Fig. 2 show characteristic peaks of cellulose I. All patterns lead to characteristic diffraction peaks of  $2\theta=14.6^\circ$  (1-10),  $16.7^\circ$  (110),  $22.8^\circ$  (200),  $34.2^\circ$  (004), who confirmed that a type I crystal lattice of natural cellulose (native cellulose) remains after chemical treatment (French, 2014; Pratama *et al.*, 2019). The peak at  $2\theta=22.8^\circ$  was associated with the crystal structure of cellulose I for all samples, while the amorphous background was characterized by an intensity at  $2\theta$  around the value of  $18^\circ$  (Sucaldito and Camacho, 2017). Based on the XRD pattern obtained, there is only cellulose I with ClaNC which is mostly composed of cellulose I (Mihriyan *et al.*, 2007; Xiang *et al.*, 2016).

The percentages of crystallinity index of raw algae, bleaching-alkali treatment and ClaNC obtained were 58.8, 90.3 and 94.0%, respectively (Eq. 1). This increase in crystallization index indicates the success of hemicellulose and lignin removal stage. The values obtained correspond to the fraction of cellulose with a minimum crystallinity index of 91.5%. A special feature in the highly crystalline cellulose XRD pattern is expressed by narrow peaks centered at values of  $2\theta$  around  $14.6^\circ$  and  $16.8^\circ$ , indicating the specific uniplanar orientation of *Cladophora* cellulose (France, 2014; Mihriyan, 2011; Wada *et al.*, 2003; Wada and Okano, 2001). Peak-1 at  $2\theta=14.6^\circ$  corresponds to the lattice planes I $\alpha$  [100] and I $\beta$  [1-10], peak-2 at  $2\theta=16.8^\circ$  corresponds to the planes I $\alpha$  [010] and I $\beta$  [110], and peak-3 at  $2\theta=22.8^\circ$  is assigned to the I $\alpha$  [110] and I $\beta$  [200] planes.

The crystallite size was calculated using Eq. 2 with wavelengths, FWHM values, and  $\theta$  obtained from XRD pattern on *Cladophora glomerata*. The calculations obtained crystallite size of 24.22, 29.35, and 31.54 nm for samples a, b, and c, respectively (Fig.

2). The crystallite size is influenced by the FWHM value; the smaller the FWHM value, the larger the crystallite size value. On the other hand, the crystal index becomes higher because the peak intensity is higher. From these data, it can be seen that acid hydrolysis treatment has successfully eliminated the amorphous domain of cellulose by increasing the cellulose crystal index. During the acid hydrolysis process, hydronium ions penetrate the amorphous region, accelerate the hydrolytic cleavage of glycosidic bonds, and release individual crystals. In addition, the growth of sample crystal size at each treatment stage is associated with the assembly of the monocrystals themselves for ClaNC forming (Sucaldito and Camacho, 2017). ClaNC rearrangement after hydrolysis treatment results in highly orderly packing and enhances the hydrogen interaction between ClaNC chains creating a crystal structure with high peak intensity. This phenomenon results in sharper diffraction peaks in the XRD pattern (Fig. 2).

#### Morphology of cellulose *Cladophora*

In general, the morphology of the surface structure of the *Cladophora* samples (Fig. 3) showed differences in size and physical shape (Fig. 3a). This difference occurs due to the removal of some components of the raw material after bleaching and alkali treatment (Fig. 3b) to form fine but agglomerated microfibril features. Microfibrils begin to form threads that are interconnected with each other like a web structure but a larger surface area. HCl hydrolysis treatment clarified the structure of the nanofibrils, as shown in the SEM figure at higher magnification (Fig. 3c). The morphology formed is consistent with studies on the structure of

*Cladophora* cellulose (Xiang *et al.*, 2016; Mihranyan, 2011).

The morphology and size distribution of ClaNC were characterized using TEM. Nano-sized ClaNCs were clearly observed on TEM images (Fig. 4) with elongated nanorods. TEM analysis (Fig. 4), showed that *Cladophora glomerata* reached the nanoscale with a very high aspect ratio. The diameter distribution is approximately 30.6 ( $\pm 0.85$ ) nm and the average length is 333.8 ( $\pm 8.2$ ) nm. The aspect ratio of nanofiber was found to be around 10.9 nm. The similarity of these values is close to studies performed on *Cladophora rupestris* (Sucaldito and Camacho, 2017; Kalashnikova *et al.*, 2013) using HCl for hydrolysis treatment. The dominant ClaNC size

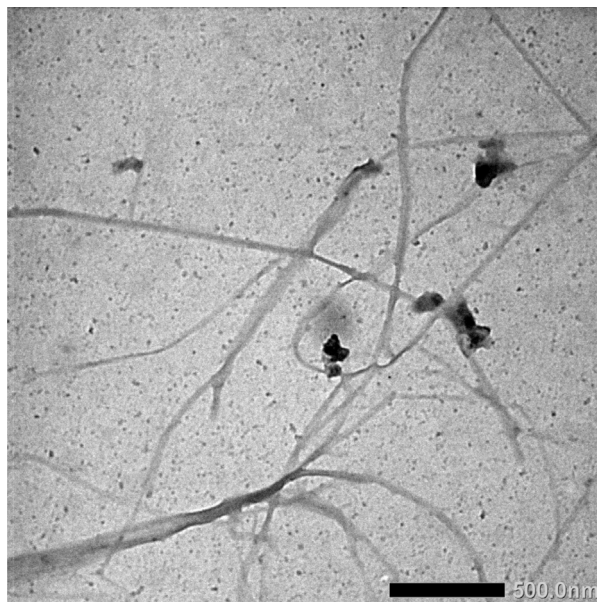


Fig. 4. TEM micrograph of *Cladophora* cellulose prepared by HCl treatment

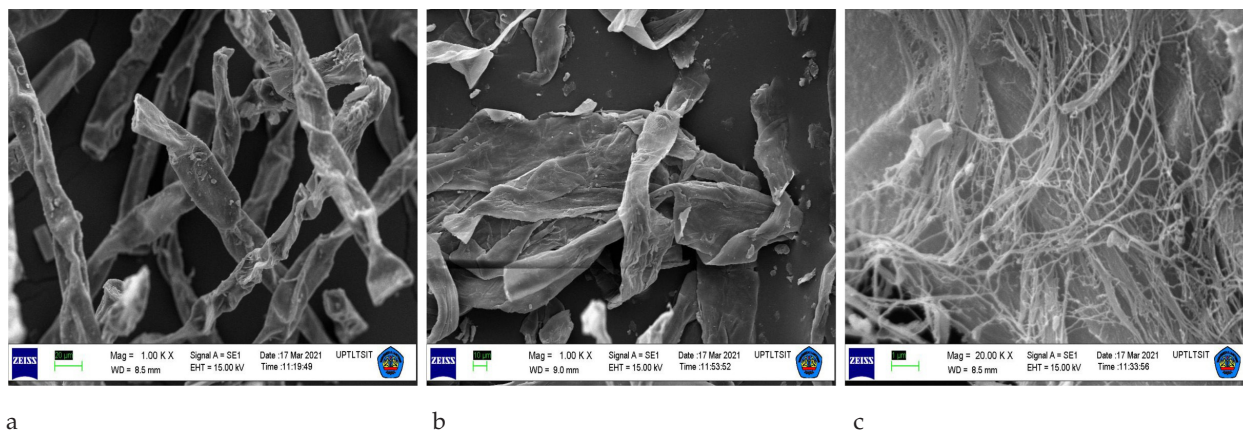


Fig. 3. Morphology surface of SEM images (a) raw material, (b) bleach-alkali-treatment, (c) ClaNC from *Cladophora* sp.

is generally less than 500 nm in length, and about 10 to 30 nm wide/diameter. Combining the results from the XRD pattern and SEM/TEM images proved the success of the acid hydrolysis (HCl) process on microcellulose. Acid protons have invaded and removed amorphous regions in the cellulose structure and maintained its crystal structure. This causes the ClaNc crystal index to be higher, and the ClaNc length to be shorter.

## Conclusion

Nanocellulose from *Cladophora glomerata*, freshwater green algae from riverside, was synthesized and extracted using HCl hydrolysis. Changes in chemical composition in each step of *Cladophora* extraction were observed using FTIR. The SEM and TEM images showed a web-like network of nanocrystals whose diameter is 30.6 ( $\pm 0.85$ ) nm. ClaNc is highly crystalline (94.0% crystallinity index) in terms of XRD pattern with plane orientation  $1\alpha$  [110] and  $1\beta$  [200].

## Acknowledgement

This work supported by a research grant of Doctoral Program, by Ministry of Education, Culture, Research and Technology of the Republic of Indonesia. Acknowledgments to research institutes and community service, University of Lampung.

## References

- Abraham, E., Deepa, B., Pothan, L. A., Jacob, M., Thomas, S., Cvelbar, U. and Anandjiwala, R. 2011. Extraction of nanocellulose fibrils from lignocellulosic fibres: A novel approach. *Carbohydrate Polymers*. 86(4): 1468–1475. <https://doi.org/10.1016/j.carbpol.2011.06.034>
- Bagheri, S., Julkapli, N. M. and Mansouri, N. 2017. Nanocrystalline Cellulose/ : Green , Multifunctional and Sustainable Nanomaterials. In: *Handbook of Composites from Renewable Materials*. 7 : 523–556). Scrivener Publishing LLC.
- Beads, C. C., Rocha, I., Hattori, Y., Diniz, M., Mihranyan, A., Strømme, M. and Lindh, J. 2018. Spectroscopic and Physico-chemical Characterization of Sulfonated *Cladophora* Cellulose Beads [Research-article]. *Langmuir*. 34 (August) : 11121–11125. <https://doi.org/10.1021/acs.langmuir.8b01704>
- Brinchi, L., Cotana, F., Fortunati, E. and Kenny, J.M. 2013. Production of nanocrystalline cellulose from lignocellulosic biomass: Technology and applications. *Carbohydrate Polymers*. 94 (1) : 154–169. <https://doi.org/10.1016/j.carbpol.2013.01.033>
- Camacho, D.H., Gerongay, S.R.A.E.C. and Macalinao, J.P.C. 2013. *Cladophora* Cellulose – Polyaniline Composite For Remediation Of Toxic Chromium (VI). *Cellulose Chem. Technol.* 47(1–2) : 125–132.
- Dufresne, A. 2013. Nanocellulose/ : a new ageless bionanomaterial. *Materials Today*. 16(6) : 220–227. <https://doi.org/10.1016/j.mattod.2013.06.004>
- French, A. D. 2014. Idealized powder diffraction patterns for cellulose polymorphs. *Cellulose*. 21(2) : 885–896. <https://doi.org/10.1007/s10570-013-0030-4>
- Fuller, M. E., Andaya, C. and McClay, K. 2018. Evaluation of ATR-FTIR for analysis of bacterial cellulose impurities. *Journal of Microbiological Methods*. 144(October 2017) : 145–151. <https://doi.org/10.1016/j.mimet.2017.10.017>
- George, M. and Montemagno, C. 2017. Cellulose Based Materials/ : in-Depth Property Survey And Assessment. *International Refereed Journal of Engineering and Science*. 6(5) : 55–76. <http://www.irjes.com/Papers/vol6-issue5/16515576.pdf>
- Giese, M., Blusch, L. K., Khan, M. K. and MacLachlan, M. J. 2015. Functional materials from cellulose-derived liquid-crystal templates. *Angewandte Chemie - International Edition*. 54(10) : 2888–2910. <https://doi.org/10.1002/anie.201407141>
- Habibi, Y., Lucia, L. A. and Rojas, O. J. 2010. Cellulose nanocrystals: Chemistry, self-assembly, and applications. *Chemical Reviews*. 110(6) : 3479–3500. <https://doi.org/10.1021/cr900339w>
- Hua, K., Carlsson, D. O., Ålander, E., Lindström, T., Strømme, M., Mihranyan, A. and Ferraz, N. 2014. Translational study between structure and biological response of nanocellulose from wood and green algae. *RSC Advances*. 4(6) : 2892–2903. <https://doi.org/10.1039/c3ra45553j>
- Jagadeesh, D., Jeevan Prasad Reddy, D. and Varada Rajulu, A. 2011. Preparation and Properties of Biodegradable Films from Wheat Protein Isolate. *Journal of Polymers and the Environment*. 19(1): 248–253. <https://doi.org/10.1007/s10924-010-0271-3>
- Kalashnikova, I., Bizot, H., Bertocini, P., Cathala, B. and Capron, I. 2013. Cellulosic nanorods of various aspect ratios for oil in water Pickering emulsions. *Soft Matter*. 9(3) : 952–959. <https://doi.org/10.1039/c2sm26472b>
- Kallel, F., Bettaieb, F., Khiari, R., García, A., Bras, J. and Chaabouni, S. E. 2016. Isolation and structural characterization of cellulose nanocrystals extracted from garlic straw residues. *Industrial Crops and Products*, 87: 287–296. <https://doi.org/10.1016/j.indcrop.2016.04.060>
- Karim, M. Z., Chowdhury, Z. Z., Hamid, S. B. A. and Ali, M. E. 2014. Statistical optimization for acid hydroly-

- sis of microcrystalline cellulose and its physiochemical characterization by using metal ion catalyst. *Materials*. 7(10): 6982–6999. <https://doi.org/10.3390/ma7106982>
- Keshavarzi, N., Mashayekhy Rad, F., Mace, A., Ansari, F., Akhtar, F., Nilsson, U., Berglund, L. and Bergström, L. 2015. Nanocellulose-Zeolite Composite Films for Odor Elimination. *ACS Applied Materials and Interfaces*. 7(26) : 14254–14262. <https://doi.org/10.1021/acsami.5b02252>
- Lee, H. J., Lee, H. S., Seo, J., Kang, Y. H., Kim, W. and Kang, T. H. K. 2019. State-of-the-art of cellulose nanocrystals and optimal method for their dispersion for construction-related applications. *Applied Sciences (Switzerland)*. 9(3) : 1–14. <https://doi.org/10.3390/app9030426>
- Mihrianyan, A. 2011. Cellulose from Cladophorales Green Algae : From Environmental Problem to High-Tech Composite Materials. *Journal of Applied Polymer Science*. 119 : 2449–2460. <https://doi.org/10.1002/app>
- Mihrianyan, A., Edsman, K. and Strømme, M. 2007. Rheological properties of cellulose hydrogels prepared from Cladophora cellulose powder. *Food Hydrocolloids*. 21(2) : 267–272. <https://doi.org/10.1016/j.foodhyd.2006.04.003>
- Moberg, T., Sahlén, K., Yao, K., Geng, S., Westman, G., Zhou, Q., Oksman, K. and Rigdahl, M. 2017. Rheological properties of nanocellulose suspensions: effects of fibril/particle dimensions and surface characteristics. *Cellulose*. 24(6): 2499–2510. <https://doi.org/10.1007/s10570-017-1283-0>
- Moon, R. J., Martini, A., Nairn, J., Youngblood, J., Martini, A. and Nairn, J. 2011. *Chem Soc Rev Cellulose nanomaterials review : structure, properties and nanocomposites*. <https://doi.org/10.1039/c0cs00108b>
- Moreno, G., Ramirez, K., Esquivel, M. and Jimenez, G. 2018. Isolation and Characterization of Nanocellulose Obtained from Industrial Crop Waste Resources by Using Mild Acid Hydrolysis. 6(4) : 362–369. <https://doi.org/10.7569/JRM.2017.634>
- Mun, S., Kim, H. C., Ko, H., Zhai, L., Kim, J. W. and Kim, J. 2017. Flexible cellulose and ZnO hybrid nanocomposite and its UV sensing characteristics. *Science and Technology of Advanced Materials*. 18(1) : 1–10. <https://doi.org/10.1080/14686996.2017.1336642>
- Nandi, S. and Guha, P. 2018. A Review on Preparation and Properties of Cellulose Nanocrystal-Incorporated Natural Biopolymer. *Journal of Packaging Technology and Research*. 2(2): 149–166. <https://doi.org/10.1007/s41783-018-0036-3>
- Pereira, P. H. F., Ornaghi Júnior, H. L., Coutinho, L. V., Duchemin, B. and Cioffi, M. O. H. 2020. Obtaining cellulose nanocrystals from pineapple crown fibers by free-chlorite hydrolysis with sulfuric acid: physicochemical and structural characterization. *Cellulose*. 27(10) : 5745–5756. <https://doi.org/10.1007/s10570-020-03179-6>
- Pratama, A. W., Piluharto, B., Indarti, D., Haryati, T. and Addy, H. S. 2019. Pengaruh Konsentrasi Asam Terhadap Sifat Fisik dan Muatan Permukaan Selulosa Termodifikasi. *ALCHEMY Jurnal Penelitian Kimia*. 15(2) : 315. <https://doi.org/10.20961/alchemistry.15.2.33756.315-328>
- Sucaldito, M. R. and Camacho, D. H. 2017. Characteristics of unique HBr-hydrolyzed cellulose nanocrystals from freshwater green algae (*Cladophora rupestris*) and its reinforcement in starch-based film. *Carbohydrate Polymers*. 169 : 315–323. <https://doi.org/10.1016/j.carbpol.2017.04.031>
- Suciyati, S. W., Manurung, P., Sembiring, S. and Situmeang, R. 2021. Comparative study of *Cladophora* sp. cellulose by using FTIR and XRD. *Journal of Physics: Conference Series*. 1751(1). <https://doi.org/10.1088/1742-6596/1751/1/012075>
- Tayeb, A. H., Amini, E., Ghasemi, S. and Tajvidi, M. 2018. Cellulose Nanomaterials — Binding Properties and Applications / : A Review. *Molecules*. 23(2684) : 1–24. <https://doi.org/10.3390/molecules23102684>
- Trache, D., Khimeche, K., Mezroua, A. and Benziane, M. 2016. Physicochemical properties of microcrystalline nitrocellulose from Alfa grass fibres and its thermal stability. *Journal of Thermal Analysis and Calorimetry*. 124(3): 1485–1496. <https://doi.org/10.1007/s10973-016-5293-1>
- Wada, M., Kondo, T. and Okano, T. 2003. Thermally induced crystal transformation from cellulose I $\alpha$  to I $\beta$ . *Polymer Journal*. 35(2): 155–159. <https://doi.org/10.1295/polymj.35.155>
- Wada, M. and Okano, T. 2001. Localization of I $\alpha$  and I $\beta$  phases in algal cellulose revealed by acid treatments. *Cellulose*. 8(3) : 183–188. <https://doi.org/10.1023/A:1013196220602>
- Xiang, Z., Gao, W., Chen, L., Lan, W. and Troy, J. Y. Z. 2016. A comparison of cellulose nanofibrils produced from *Cladophora glomerata* algae and bleached eucalyptus pulp. *Cellulose*. 23(1) : 493–503. <https://doi.org/10.1007/s10570-015-0840-7>
- Zhou, S., Nyholm, L., Strømme, M. and Wang, Z. 2019. *Cladophora Cellulose : Unique Biopolymer Nanofibrils for Emerging Energy , Cladophora Cellulose : Unique Biopolymer Nano fibrils for Emerging Energy, Environmental, and Life Science Applications*. *Acc. Chem. Res*. 52(8) : 2232–2243, 52(July), 2232–2243. <https://doi.org/10.1021/acs.accounts.9b00215>
- Zhu, J. Y., Sabo, R. and Luo, X. 2011. Integrated production of nano-fibrillated cellulose and cellulosic biofuel (ethanol) by enzymatic fractionation of wood fibers. *Green Chemistry*. 13(5): 1339–1344. <https://doi.org/10.1039/c1gc15103g>